Eur. Phys. J. C 7, 185–195 (1999)
DOI 10.1007/s100529800995

THE EUROPEAN PHYSICAL JOURNAL C
© Springer-Verlag 1999

Electroweak radiative corrections to polarized Møller scattering at high energies

A. Denner[1], S. Pozzorini[2]

[1] Paul Scherrer Institut, CH-5232 Villigen PSI, Switzerland (e-mail: Ansgar.Denner@psi.ch)
[2] Institut für Theoretische Physik, ETH-Hönggerberg, CH-8093 Zürich, Switzerland

Received: 22 July 1998 / Published online: 8 September 1998

Abstract. The cross section for $e^-e^- \to e^-e^-$ with arbitrary electron polarizations is calculated within the Electroweak Standard Model for energies large compared to the electron mass, including the complete virtual and soft-photonic $O(\alpha)$ radiative corrections. The relevant analytical results are listed, and a numerical evaluation is presented for the unpolarized and polarized cross sections as well as for polarization asymmetries. The relative weak corrections are typically of the order of 10%. At low energies, the bulk of the corrections is due to the running of the electromagnetic coupling constant. For left-handed electrons, at high energies the vertex and box corrections involving virtual W bosons become very important. The polarization asymmetry is considerably reduced by the weak radiative corrections.

1 Introduction

The linear electron colliders of the next generation will allow experiments with highly polarized electron and photon beams starting from a centre-of-mass energy of a few hundred GeV up to the TeV range. The high degree of polarization combined with a large luminosity provides a powerful tool for suppressing backgrounds and sorting out interesting physical effects. The main goal of these experiments is the search for new phenomena both directly and indirectly via precision measurements of standard quantities.

The study of Møller scattering [1], $e^-e^- \to e^-e^-$, offers some particularly interesting possibilities owing to its large cross section, which leads to very good statistics. On the one hand, small angle Møller scattering can be used as a luminosity monitor just as Bhabha scattering in e^+e^- colliders. On the other hand, the measurement of parity-violating Møller asymmetries can be employed for a very precise determination of the weak mixing angle [2,3]. Note that in contrast to the measurement of the effective mixing angle at the Z-boson resonance, the Møller asymmetries do not determine the mixing angle directly. In higher orders, it can only be extracted from the measured asymmetries if the other parameters of the Electroweak Standard Model are kept fixed. Based on the lowest-order expressions, Cuypers and Gambino [2] have shown that $\Delta \sin^2\theta_w = \pm 0.0001$ may be possible at a 2 TeV collider with 90% electron-beam polarization and detector acceptance down to about 5°. Simultaneously these measurements enable a determination of the polarization degree of the electron beams competitive with Compton polarimetry with a relative precision below one per cent. This provides an important input for other precision experiments.

In order to achieve comparable accuracy in experimental measurements and theoretical predictions, radiative corrections to Møller scattering have to be taken into account. Within QED, these corrections have been calculated for the unpolarized cross section in [4] and for polarized electrons in [5]. The electromagnetic corrections to Møller scattering within the Electroweak Standard Model, i.e. including the Z-boson-exchange diagrams, have been analysed in [6,7]. The full electroweak corrections have so far only been calculated at low energies $\sqrt{s} \ll M_Z$ [8]. In this case, corrections of -40% have been found for the polarization asymmetry.

In this paper we present the complete virtual and soft photonic $\mathcal{O}(\alpha)$ electroweak radiative corrections, which have been obtained by applying crossing symmetry to the results for Bhabha scattering calculated in [9]. As in [9], we do not discuss hard-photon corrections and neglect the electron mass wherever possible. Our results are valid for arbitrary polarizations of the external electrons.

The paper is organized as follows: In Sect. 2 we fix our notation, review the lowest-order predictions and define polarization asymmetries. In Sects. 3 and 4 we give all analytical results for the electromagnetic and weak radiative corrections. Numerical results for the radiative corrections are presented and discussed in Sect. 5.

2 Lowest-order predictions

2.1 Lowest-order cross sections

We discuss, in the framework of the Electroweak Standard Model [10], Møller scattering at high energies ($\sqrt{s} \gg m_e$). The momenta of the incoming and outgoing electrons are

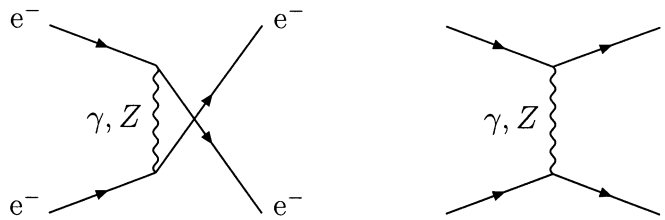

Fig. 1. Born diagrams

denoted by p_1, p_2 and q_1, q_2, the corresponding helicities by λ_1, λ_2 and σ_1, σ_2, respectively. Instead of using the proper values $\pm 1/2$ we indicate the electron helicities simply by $\pm$ or by R, L.

In the centre-of-mass (CM) system the momenta read

$$\begin{aligned} p_1^\mu &= (E,0,0,E), \quad q_1^\mu = (E, E\sin\vartheta, 0, E\cos\vartheta), \\ p_2^\mu &= (E,0,0,-E), \quad q_2^\mu = (E, -E\sin\vartheta, 0, -E\cos\vartheta), \end{aligned} \tag{2.1}$$

where E denotes the energy of the electrons and ϑ the scattering angle. The Mandelstam variables are given by

$$\begin{aligned} s &= (p_1+p_2)^2 = (q_1+q_2)^2 = 4E^2, \\ t &= (p_1-q_1)^2 = (p_2-q_2)^2 = -s\frac{1-\cos\vartheta}{2}, \\ u &= (p_1-q_2)^2 = (p_2-q_1)^2 = -s\frac{1+\cos\vartheta}{2}. \end{aligned} \tag{2.2}$$

The interaction of the electrons with the vector bosons $\gamma, \mathrm{Z}, \mathrm{W}$ is described by left- and right-handed coupling constants g_λ^i:

$$\begin{aligned} &g_\pm^\gamma = 1, \qquad g_-^Z = \frac{2s_\mathrm{w}^2-1}{2s_\mathrm{w}c_\mathrm{w}}, \qquad g_+^Z = \frac{s_\mathrm{w}}{c_\mathrm{w}}, \\ &g_-^W = \frac{1}{\sqrt{2}\,s_\mathrm{w}}, \qquad g_+^W = 0, \end{aligned} \tag{2.3}$$

with

$$c_\mathrm{w} = \frac{M_\mathrm{W}}{M_\mathrm{Z}}, \qquad s_\mathrm{w} = \sqrt{1-c_\mathrm{w}^2}. \tag{2.4}$$

The lowest-order amplitude gets contributions from the exchange of photons and Z bosons in the u- and t-channel diagrams shown in Fig. 1. The corresponding matrix elements are denoted $\mathcal{M}^{ri}_{\mathrm{Born}}(\lambda_1,\lambda_2,\sigma_1,\sigma_2)$, with $r = u,t$ and $i = \gamma, Z$. Owing to helicity selection rules, in the ultra-relativistic limit ($s, |t|, |u| \gg m_\mathrm{e}^2$) only the following matrix elements are non-vanishing ($\lambda = \pm$):

$$\begin{aligned} \mathcal{M}^{ui}_{\mathrm{Born}}(\lambda,\lambda,\lambda,\lambda) &= \mathcal{M}_1^{ui}(\lambda) = g_\lambda^i g_\lambda^i \frac{2s}{u-M_i^2}, \\ \mathcal{M}^{ui}_{\mathrm{Born}}(\lambda,-\lambda,-\lambda,\lambda) &= \mathcal{M}_2^{ui}(\lambda) = g_+^i g_-^i \frac{2t}{u-M_i^2}, \\ \mathcal{M}^{ti}_{\mathrm{Born}}(\lambda,\lambda,\lambda,\lambda) &= \mathcal{M}_1^{ti}(\lambda) = g_\lambda^i g_\lambda^i \frac{2s}{t-M_i^2}, \\ \mathcal{M}^{ti}_{\mathrm{Born}}(\lambda,-\lambda,\lambda,-\lambda) &= \mathcal{M}_3^{ti}(\lambda) = g_+^i g_-^i \frac{2u}{t-M_i^2}. \end{aligned} \tag{2.5}$$

Summing and squaring the matrix elements yields the Born cross sections in the CM frame

$$\left(\frac{\mathrm{d}\sigma}{\mathrm{d}\Omega}\right)_{a,\mathrm{Born}}(\lambda) = \frac{\alpha^2}{4s}\Big|\sum_{r,i}\mathcal{M}^{ri}_{a,\mathrm{Born}}(\lambda)\Big|^2; \tag{2.6}$$

the index $a = 1,2,3$ corresponds to the different sets of helicities in (2.5). The cross sections for arbitrary degrees of longitudinal polarization P_1, P_2 of the incoming electrons and unpolarized outgoing electrons are obtained as

$$\left(\frac{\mathrm{d}\sigma}{\mathrm{d}\Omega}\right)(P_1,P_2) = \sum_{\lambda_1,\lambda_2}\frac{1+\lambda_1 P_1}{2}\frac{1+\lambda_2 P_2}{2}\left(\frac{\mathrm{d}\sigma}{\mathrm{d}\Omega}\right)_{\lambda_1,\lambda_2}. \tag{2.7}$$

In lowest order, the corresponding polarized cross sections are given by

$$\begin{aligned} \left(\frac{\mathrm{d}\sigma}{\mathrm{d}\Omega}\right)_{\lambda,\lambda} &= \left(\frac{\mathrm{d}\sigma}{\mathrm{d}\Omega}\right)_{1,\mathrm{Born}}(\lambda) \\ &= \frac{\alpha^2}{s}\left[\sum_i \left(g_\lambda^i\right)^2\left(\frac{s}{u-M_i^2}+\frac{s}{t-M_i^2}\right)\right]^2, \\ \left(\frac{\mathrm{d}\sigma}{\mathrm{d}\Omega}\right)_{\lambda,-\lambda} &= \sum_{a=2,3}\left(\frac{\mathrm{d}\sigma}{\mathrm{d}\Omega}\right)_{a,\mathrm{Born}}(\lambda) \\ &= \frac{\alpha^2}{s}\left[\left(\sum_i g_-^i g_+^i \frac{t}{u-M_i^2}\right)^2\right. \\ &\qquad \left. + \left(\sum_i g_-^i g_+^i \frac{u}{t-M_i^2}\right)^2\right]. \end{aligned} \tag{2.8}$$

Notice that for equal polarizations of the incoming electrons (RR or LL) the u- and t-channel matrix elements interfere, whereas in the other case (RL or LR) no such interference exists.

As a consequence of rotational invariance, the RL and LR cross sections are equal. Furthermore, the polarized cross sections (2.8) are symmetric with respect to $\vartheta = 90^\circ$ owing to presence of two identical fermions in the final state. These symmetries hold to all orders of perturbation theory.

For $|t|, |u| \gg M_\mathrm{Z}^2$ the polarized cross sections take the simple form

$$\begin{aligned} \left(\frac{\mathrm{d}\sigma}{\mathrm{d}\Omega}\right)_{\mathrm{RR}} &\sim \frac{\alpha^2}{s}\frac{16}{c_\mathrm{w}^4}\frac{1}{\sin^4\vartheta}, \\ \left(\frac{\mathrm{d}\sigma}{\mathrm{d}\Omega}\right)_{\mathrm{LL}} &\sim \frac{1}{16 s_\mathrm{w}^4}\left(\frac{\mathrm{d}\sigma}{\mathrm{d}\Omega}\right)_{\mathrm{RR}}, \\ \left(\frac{\mathrm{d}\sigma}{\mathrm{d}\Omega}\right)_{\mathrm{LR}} &\sim \frac{(1-\cos\vartheta)^4+(1+\cos\vartheta)^4}{64}\left(\frac{\mathrm{d}\sigma}{\mathrm{d}\Omega}\right)_{\mathrm{RR}}. \end{aligned} \tag{2.9}$$

The integrated cross section is given by

$$\sigma = \frac{1}{2}\int \mathrm{d}\Omega\left(\frac{\mathrm{d}\sigma}{\mathrm{d}\Omega}\right) = \int_{\cos\vartheta>0}\mathrm{d}\Omega\left(\frac{\mathrm{d}\sigma}{\mathrm{d}\Omega}\right), \tag{2.10}$$

with the symmetry factor $1/2$ owing to the two identical electrons in the final state.

2.2 Polarization asymmetries

With polarized electron beams and the possibility to invert these polarization, four different polarized cross sections can be measured. Assuming the same luminosity $\mathcal{L}$

for all channels, the numbers of events for these polarization settings are given by:

$$
\begin{aligned}
N_{\mathrm{RR}} &= \mathcal{L} \int \mathrm{d}\Omega \left(\frac{\mathrm{d}\sigma}{\mathrm{d}\Omega}\right)(+P_1,+P_2),\\
N_{\mathrm{RL}} &= \mathcal{L} \int \mathrm{d}\Omega \left(\frac{\mathrm{d}\sigma}{\mathrm{d}\Omega}\right)(+P_1,-P_2),\\
N_{\mathrm{LR}} &= \mathcal{L} \int \mathrm{d}\Omega \left(\frac{\mathrm{d}\sigma}{\mathrm{d}\Omega}\right)(-P_1,+P_2),\\
N_{\mathrm{LL}} &= \mathcal{L} \int \mathrm{d}\Omega \left(\frac{\mathrm{d}\sigma}{\mathrm{d}\Omega}\right)(-P_1,-P_2),
\end{aligned}
\tag{2.11}
$$

where the integral extends over a suitable volume of phase space.

From these four event rates, three independent asymmetries can be formed [2,3]. A particularly suitable set consists of

$$
\begin{aligned}
\frac{N_{\mathrm{LL}}+N_{\mathrm{LR}}-N_{\mathrm{RL}}-N_{\mathrm{RR}}}{N_{\mathrm{LL}}+N_{\mathrm{LR}}+N_{\mathrm{RL}}+N_{\mathrm{RR}}} &= P_1 A_{\mathrm{LR}}^{(1)},\\
\frac{N_{\mathrm{LL}}+N_{\mathrm{RL}}-N_{\mathrm{LR}}-N_{\mathrm{RR}}}{N_{\mathrm{LL}}+N_{\mathrm{LR}}+N_{\mathrm{RL}}+N_{\mathrm{RR}}} &= P_2 A_{\mathrm{LR}}^{(1)},\\
\sqrt{\frac{(N_{\mathrm{LL}}-N_{\mathrm{RR}})^2-(N_{\mathrm{RL}}-N_{\mathrm{LR}})^2}{(N_{\mathrm{LL}}+N_{\mathrm{RR}})^2-(N_{\mathrm{LR}}+N_{\mathrm{RL}})^2}} &= A_{\mathrm{LR}}^{(2)}.
\end{aligned}
\tag{2.12}
$$

The asymmetry functions

$$
A_{\mathrm{LR}}^{(1)} = \frac{\sigma_{\mathrm{LL}}-\sigma_{\mathrm{RR}}}{\sigma_{\mathrm{LL}}+2\sigma_{\mathrm{LR}}+\sigma_{\mathrm{RR}}} \tag{2.13}
$$

and

$$
A_{\mathrm{LR}}^{(2)} = \frac{|\sigma_{\mathrm{LL}}-\sigma_{\mathrm{RR}}|}{\sqrt{(\sigma_{\mathrm{LL}}+\sigma_{\mathrm{RR}})^2-(2\sigma_{\mathrm{LR}})^2}} \tag{2.14}
$$

are independent of the polarization degrees. Moreover, for scattering angles near to $\vartheta = 90^\circ$ where σ_{LR} is suppressed with respect to σ_{LL} and σ_{RR}, $A_{\mathrm{LR}}^{(1)}$ and $A_{\mathrm{LR}}^{(2)}$ are roughly equal to

$$
A_{\mathrm{LR}}^{(3)} = \frac{\sigma_{\mathrm{LL}}-\sigma_{\mathrm{RR}}}{\sigma_{\mathrm{LL}}+\sigma_{\mathrm{RR}}}. \tag{2.15}
$$

All asymmetry functions $A_{\mathrm{LR}}^{(k)}$, $k = 1,2,3$, are proportional to

$$
\sigma_{\mathrm{LL}}-\sigma_{\mathrm{RR}} \propto \left(g_-^Z\right)^2 - \left(g_+^Z\right)^2 \propto 1-4s_{\mathrm{w}}^2, \tag{2.16}
$$

and, owing to $s_{\mathrm{w}}^2 \approx 0.23 \sim 1/4$, they are very sensitive to small variations of the weak mixing angle.

The set of asymmetries defined in (2.12) is particularly useful in order to determine the polarization degrees of the two electron beams and the weak mixing angle. In the third asymmetry the polarization degrees drop out, and the weak mixing angle can be directly determined. Then $A_{\mathrm{LR}}^{(1)}$ is fixed and the first two asymmetries can be used to measure directly the polarization degrees.

3 Electromagnetic radiative corrections

Using crossing symmetry, the one-loop radiative corrections to Møller scattering can be directly obtained from the results for Bhabha scattering listed in [9]. The corresponding Feynman diagrams result from those given in [9] via crossing. The results of [9] have been obtained within the on-shell renormalization scheme [11] with the fine-structure constant α and the masses M_{W}, M_{Z}, M_{H} and m_f as physical parameters.

In the ultra-relativistic limit the amplitudes for the virtual corrections factorize into Born matrix elements and correction factors ($r = u,t$; $i = \gamma, Z$; $a = 1,2,3$)

$$
\mathcal{M}_{a,\mathrm{virt}}^{ri}(\lambda) = \mathcal{M}_a^{ri}(\lambda)\delta_{a,\mathrm{virt}}^{ri}(\lambda). \tag{3.1}
$$

The virtual corrections can be split into electromagnetic and weak corrections

$$
\delta_{a,\mathrm{virt}}^{ri}(\lambda) = \delta_{a,\mathrm{em,virt}}^{ri}(\lambda) + \delta_{a,\mathrm{w,virt}}^{ri}(\lambda). \tag{3.2}
$$

Note that we define this splitting differently from [9]. Into the electromagnetic corrections we include only those diagrams (and the corresponding counterterms) that arise from the Born matrix elements by adding a photon line; all other corrections are considered as weak corrections. In contrast to [9] the fermionic loops contained in the photon self-energy are included in the weak corrections.

3.1 Electromagnetic virtual corrections

The electromagnetic virtual corrections consist of vertex (V) and box diagrams (B) with virtual photons

$$
\delta_{a,\mathrm{em,virt}}^{ri}(\lambda) = \delta_{a,\mathrm{em,V}}^{ri}(\lambda) + \delta_{a,\mathrm{em,B}}^{ri}(\lambda). \tag{3.3}
$$

The corresponding amplitudes are infrared (IR)-divergent. The IR singularities are regularized by an infinitesimal photon mass μ.

For each vertex in the Born diagrams there is a vertex-correction diagram. The corresponding correction factors read

$$
\delta_{a,\mathrm{em,V}}^{ri}(\lambda) = 2F_{\mathrm{em}}(r), \tag{3.4}
$$

with the electromagnetic form factor F_{em} given in [9]. Each Born diagram with photon-exchange gives rise to two box diagrams with double photon exchange and correction factors

$$
\delta_{\substack{1\\2},\mathrm{em,B}}^{u\gamma}(\lambda) = C_\pm^{\gamma\gamma}(u,t), \quad \delta_{\substack{1\\3},\mathrm{em,B}}^{t\gamma}(\lambda) = C_\pm^{\gamma\gamma}(t,u), \tag{3.5}
$$

and for each Born diagram with Z-boson exchange four box diagrams with Z-boson and photon exchange and correction factors exist

$$
\delta_{\substack{1\\2},\mathrm{em,B}}^{uZ}(\lambda) = C_\pm^{\gamma Z}(u,t), \quad \delta_{\substack{1\\3},\mathrm{em,B}}^{tZ}(\lambda) = C_\pm^{\gamma Z}(t,u). \tag{3.6}
$$

The analytical expressions for the electromagnetic box functions $C_\pm^{\gamma\gamma}(s,t)$ and $C_\pm^{\gamma Z}(s,t)$ can be found in [9]. To make correct use of these results, recall that the Mandelstam variables are related by $s+t+u = 0$ in the ultra-relativistic limit.

3.2 Soft-photon bremsstrahlung

In order to obtain an IR-finite cross section one has to add real bremsstrahlung. In the soft-photon limit, i.e. restricting the energy of the emitted photon by $k^0 \leq \Delta E \ll \sqrt{s}$, the corresponding cross section factorizes into the lowest-order cross section and a correction factor

$$\left(\frac{\mathrm{d}\sigma}{\mathrm{d}\Omega}\right)_{a,\mathrm{brems}}(\lambda) = \delta_{\mathrm{brems}} \left(\frac{\mathrm{d}\sigma}{\mathrm{d}\Omega}\right)_{a,\mathrm{Born}}(\lambda) \tag{3.7}$$

with

$$\delta_{\mathrm{brems}} = \frac{\alpha}{\pi}\Bigg\{4\ln\frac{2\Delta E}{\mu}\left[\ln\frac{ut}{sm_\mathrm{e}^2}-1\right]-\left[\ln\frac{s}{m_\mathrm{e}^2}-1\right]^2 +1-\frac{2\pi^2}{3}+X\Bigg\}, \tag{3.8}$$

and

$$X = \left(\ln\frac{u}{t}\right)^2 + \frac{\pi^2}{3}. \tag{3.9}$$

Note that, owing to the condition $k_0 \leq \Delta E$, this result is frame-dependent and cannot be directly obtained from the corresponding result for Bhabha scattering via crossing symmetry.

3.3 Corrections to the polarized cross sections

The virtual $\mathcal{O}(\alpha)$ corrections to the polarized cross sections (2.6) are given by the interference terms between lowest-order and one-loop matrix elements

$$\begin{aligned}\Delta\left(\frac{\mathrm{d}\sigma}{\mathrm{d}\Omega}\right)_{a,\mathrm{em,virt}}(\lambda) &= \frac{\alpha^2}{4s}\sum_{r,i}\sum_{r',i'}\mathrm{Re}\Big\{\mathcal{M}_a^{ri}(\lambda)(\mathcal{M}_a^{r'i'}(\lambda))^* \\ &\quad\times\left[\delta^{ri}_{a,\mathrm{em,virt}}(\lambda)+(\delta^{r'i'}_{a,\mathrm{em,virt}}(\lambda))^*\right]\Big\}.\end{aligned} \tag{3.10}$$

After adding the soft-photon bremsstrahlung cross section, the total IR-finite $O(\alpha)$ electromagnetic corrections can be written as follows:

$$\begin{aligned}\Delta\left(\frac{\mathrm{d}\sigma}{\mathrm{d}\Omega}\right)_{a,\mathrm{em}}(\lambda) &= \Delta\left(\frac{\mathrm{d}\sigma}{\mathrm{d}\Omega}\right)_{a,\mathrm{em,virt}}(\lambda)+\left(\frac{\mathrm{d}\sigma}{\mathrm{d}\Omega}\right)_{a,\mathrm{brems}}(\lambda) \\ &= \frac{\alpha^2}{4s}\sum_{r,i}\sum_{r',i'}\mathrm{Re}\Big\{\mathcal{M}_a^{ri}(\lambda)(\mathcal{M}_a^{r'i'}(\lambda))^* \\ &\quad\times\left[\delta^{ri}_{a,\mathrm{em}}(\lambda)+(\delta^{r'i'}_{a,\mathrm{em}}(\lambda))^*+\gamma\right]\Big\},\end{aligned} \tag{3.11}$$

with[1]

$$\begin{aligned}\delta^{u\gamma}_{\substack{1\\2},\mathrm{em}}(\lambda) &= \frac{\alpha}{2\pi}\left[Z+Y(u)+X\right]\pm 2I_5^{\gamma\gamma}\left(u,\begin{smallmatrix}t\\s\end{smallmatrix}\right),\\ \delta^{t\gamma}_{\substack{1\\3},\mathrm{em}}(\lambda) &= \frac{\alpha}{2\pi}\left[Z+Y(t)+X\right]\pm 2I_5^{\gamma\gamma}\left(t,\begin{smallmatrix}u\\s\end{smallmatrix}\right),\\ \delta^{uZ}_{\substack{1\\2},\mathrm{em}}(\lambda) &= \frac{\alpha}{2\pi}\left[Z+Y(u)+X+2D(u,t)\right]\\ &\quad\pm 4I_5^{\gamma Z}\left(u,\begin{smallmatrix}t\\s\end{smallmatrix}\right),\\ \delta^{tZ}_{\substack{1\\3},\mathrm{em}}(\lambda) &= \frac{\alpha}{2\pi}\left[Z+Y(t)+X+2D(t,u)\right]\\ &\quad\pm 4I_5^{\gamma Z}\left(t,\begin{smallmatrix}u\\s\end{smallmatrix}\right),\end{aligned} \tag{3.12}$$

and the cut-off-dependent factor

$$\gamma = 4\frac{\alpha}{\pi}\ln\frac{2\Delta E}{\sqrt{s}}\left[\ln\frac{ut}{sm_\mathrm{e}^2}-1\right]. \tag{3.13}$$

The box functions $I_5^{\gamma\gamma}(u,t)$ and $I_5^{\gamma Z}(u,t)$ are defined in [11], and the function $D(u,t)$ reads[2]

$$\begin{aligned}D(u,t) = &-\ln\frac{-t}{s}\left[\ln\frac{M_\mathrm{Z}^2-u}{-u}+\ln\frac{M_\mathrm{Z}^2-u}{M_\mathrm{Z}^2}\right]\\ &+\mathrm{Sp}\left(\frac{M_\mathrm{Z}^2+t}{t}\right)-\mathrm{Sp}\left(\frac{M_\mathrm{Z}^2+s}{s}\right)\end{aligned} \tag{3.14}$$

with the Spence function $\mathrm{Sp}(x) = -\int_0^1(\mathrm{d}t/t)\ln(1-xt)$. Furthermore, we have introduced

$$\begin{aligned}Y(r) &= -\left(\ln\frac{-r}{s}\right)^2-2\ln\frac{-r}{s}\ln\frac{r+s}{s}+3\ln\frac{-r}{s}-\pi^2,\\ Z &= 3\ln\frac{s}{m_\mathrm{e}^2}+\frac{2\pi^2}{3}-4,\end{aligned} \tag{3.15}$$

which correspond to the quantities defined in [9].

4 Weak radiative corrections

4.1 Corrections to the matrix elements

The weak radiative corrections result from self-energy (Σ), vertex (V) and box (B) diagrams

$$\delta^{ri}_{a,\mathrm{w,virt}}(\lambda) = \delta^{ri}_{a,\mathrm{w},\Sigma}(\lambda)+\delta^{ri}_{a,\mathrm{w,V}}(\lambda)+\delta^{ri}_{a,\mathrm{w,B}}(\lambda). \tag{4.1}$$

In the on-shell renormalization scheme the electron wave function is not renormalized, and the only self-energy corrections to Møller scattering come from the exchanged gauge bosons. Each photon exchange Born diagram gives rise to a photon-self-energy correction term, and each Z-boson-exchange Born diagram to three correction terms that involve the Z-self-energy, and the γ–Z and Z–γ mixing energy. The corresponding correction factors are given by

$$\begin{aligned}\delta^{r\gamma}_{a,\mathrm{w},\Sigma}(\lambda) &= \Pi^\gamma(r),\\ \delta^{rZ}_{1,\mathrm{w},\Sigma}(\lambda) &= \Pi^Z(r)+\frac{2}{g_\lambda^Z}\Pi^{\gamma Z}(r),\\ \delta^{rZ}_{\substack{2\\3},\mathrm{w},\Sigma}(\lambda) &= \Pi^Z(r)+\left(\frac{1}{g_+^Z}+\frac{1}{g_-^Z}\right)\Pi^{\gamma Z}(r),\end{aligned} \tag{4.2}$$

[1] Note that in the corresponding formula (3.24) in [9] the functions $I_5^{\gamma\gamma}(u,t)$ and $I_5^{\gamma Z}(u,t)$ should not be multiplied with $\alpha/2\pi$

[2] In the definition of this function in (3.25) in [9] the factor 2 in front of the Spence function should be removed

with

$$\Pi^{\gamma}(r) = -\frac{\Sigma^{\gamma}(r)}{r}, \qquad \Pi^{Z}(r) = -\frac{\Sigma^{Z}(r)}{r - M_{\mathrm{Z}}^2},$$
$$\Pi^{\gamma Z}(r) = -\frac{\Sigma^{\gamma Z}(r)}{r}. \tag{4.3}$$

The self-energies and mixing energies can be found in [12]. The hadronic part of the photon vacuum polarization associated with light quarks cannot be calculated reliably within perturbation theory. Instead, the contribution of the five light quarks can be directly obtained from the cross section for $\mathrm{e}^+\mathrm{e}^- \to$ hadrons via a dispersion integral [13]. We use the parameterization

$$\mathrm{Re}\,\Pi^{\gamma}_{\mathrm{had}}(s) = A + B\ln(1 + C|s|), \tag{4.4}$$

with A, B, C adjusted to a recent fit [14] of the experimental data (Note that the constants A, B, C are fixed differently in different regions).

The weak vertex corrections involve, besides contributions from the exchange of virtual Z and W bosons, a non-abelian contribution and lead to the correction factors

$$\delta^{ri}_{1,\mathrm{w,V}}(\lambda) = 2F^i_{\mathrm{w}}(r,\lambda),$$
$$\delta^{ri}_{\substack{2\\3},\mathrm{w,V}}(\lambda) = F^i_{\mathrm{w}}(r,+) + F^i_{\mathrm{w}}(r,-), \tag{4.5}$$

with the weak form factors $F^i_{\mathrm{w}}(r,\lambda)$ [9]. The weak box corrections consist of four diagrams with double Z-boson exchange and two diagrams with double W-boson exchange. By convention they are treated as corrections to the photon-exchange Born diagrams. The corresponding correction factors read

$$\delta^{u\gamma}_{1,\mathrm{w,B}}(\lambda) = (g^Z_\lambda)^4 C^{ZZ}_+(u,t) + (g^W_\lambda)^4 C^{WW}_+(u,t),$$
$$\delta^{t\gamma}_{1,\mathrm{w,B}}(\lambda) = (g^Z_\lambda)^4 C^{ZZ}_+(t,u) + (g^W_\lambda)^4 C^{WW}_+(t,u),$$
$$\delta^{u\gamma}_{2,\mathrm{w,B}}(\lambda) = (g^Z_+)^2 (g^Z_-)^2 C^{ZZ}_-(u,t),$$
$$\delta^{t\gamma}_{3,\mathrm{w,B}}(\lambda) = (g^Z_+)^2 (g^Z_-)^2 C^{ZZ}_-(t,u), \tag{4.6}$$

while $\delta^{rZ}_{a,\mathrm{w,B}}(\lambda) = 0$. The weak box functions $C^{ZZ}_{\pm}(s,t)$ and $C^{WW}_{+}(s,t)$ are given in [9] and [11].

4.2 Corrections to the polarized cross sections

The weak $\mathcal{O}(\alpha)$ corrections to the polarized cross sections (2.6) read

$$\Delta\left(\frac{\mathrm{d}\sigma}{\mathrm{d}\Omega}\right)_{a,\mathrm{w}}(\lambda) = \frac{\alpha^2}{4s}\sum_{r,i}\sum_{r',i'}\mathrm{Re}\Big\{\mathcal{M}^{ri}_a(\lambda)(\mathcal{M}^{r'i'}_a(\lambda))^* \times\Big[\delta^{ri}_{a,\mathrm{w,virt}}(\lambda) + (\delta^{r'i'}_{a,\mathrm{w,virt}}(\lambda))^*\Big]\Big\}. \tag{4.7}$$

Finally, the total $\mathcal{O}(\alpha)$ corrections to the cross section are given by

$$\Delta\left(\frac{\mathrm{d}\sigma}{\mathrm{d}\Omega}\right)_{a}(\lambda) = \Delta\left(\frac{\mathrm{d}\sigma}{\mathrm{d}\Omega}\right)_{a,\mathrm{w}}(\lambda) + \Delta\left(\frac{\mathrm{d}\sigma}{\mathrm{d}\Omega}\right)_{a,\mathrm{em}}(\lambda). \tag{4.8}$$

5 Numeric results and discussion

In the previous chapters we have summarized the analytical formulas for the polarized Møller cross section including the complete $O(\alpha)$ radiative corrections in the soft-photon approximation. Here, we present a numerical evaluation of these results obtained with the masses

$$M_{\mathrm{Z}} = 91.187\,\mathrm{GeV}, \qquad M_{\mathrm{W}} = 80.4\,\mathrm{GeV},$$
$$M_{\mathrm{H}} = 300\,\mathrm{GeV}, \qquad m_{\mathrm{t}} = 175\,\mathrm{GeV}, \tag{5.1}$$

and with the fine-structure constant $\alpha = 1/137.03604$.

Our main interest lies in the discussion of the relative weak corrections defined by $\delta_{\mathrm{w}} = \Delta\big(\frac{\mathrm{d}\sigma}{\mathrm{d}\Omega}\big)_{\mathrm{w}}/\big(\frac{\mathrm{d}\sigma}{\mathrm{d}\Omega}\big)_{\mathrm{Born}}$. These are sensitive to the complete structure of the Electroweak Standard Model and may influence the determination of the weak mixing angle from asymmetries considerably. On the other hand, the electromagnetic corrections involve only well-known physics but are sensitive to the experimental cuts for hard-photon emission. They must be included properly for specific experiments, but as far as the asymmetries are concerned, they are relatively unimportant. The soft-photon effects factorize and cancel exactly, and the same should be true for the bulk of the hard-photon effects. The remaining electromagnetic effects are mostly proportional to the lowest-order asymmetries and therefore do not give rise to large corrections. We note that the complete electromagnetic corrections for the luminosity measurement have been discussed in [6].

The weak corrections are separated in a gauge-invariant way into fermionic and bosonic parts

$$\delta_{\mathrm{w}} = \delta_{\mathrm{w,fer}} + \delta_{\mathrm{w,bos}}. \tag{5.2}$$

The fermionic part consists of all diagrams with closed fermion loops and fermionic counterterms and is, in the renormalization scheme of [11], given by the hadronic and leptonic contributions to the gauge-boson self-energies. The remaining weak corrections are called bosonic and are, within the 't Hooft–Feynman gauge, further split into self-energy, vertex, and box contributions,

$$\delta_{\mathrm{w,bos}} = \delta_{\mathrm{w,bos},\Sigma} + \delta_{\mathrm{w,bos,V}} + \delta_{\mathrm{w,bos,B}}. \tag{5.3}$$

The fermionic corrections involve, in particular, the contributions that are related to the running of the electromagnetic coupling constant α. Including only the contributions of the light fermions, we define the corresponding correction factors to the matrix elements $\mathcal{M}^{ri}_a(\lambda)$ as

$$\delta^{r\gamma}_{a,\mathrm{run}}(\lambda) = \Pi^{\gamma}_{f\neq\mathrm{top}}(r),$$
$$\delta^{rZ}_{a,\mathrm{run}}(\lambda) = \Pi^{\gamma}_{f\neq\mathrm{top}}(M_{\mathrm{Z}}^2), \qquad r = u, t. \tag{5.4}$$

Then, the fermionic corrections can be split into those related to the running of α and the remaining ones

$$\delta_{\mathrm{w,fer}} = \delta_{\mathrm{w,run}} + \delta_{\mathrm{w,fer,rem}}. \tag{5.5}$$

The different contributions to the weak corrections for the unpolarized cross section ($P_1 = P_2 = 0$) are presented

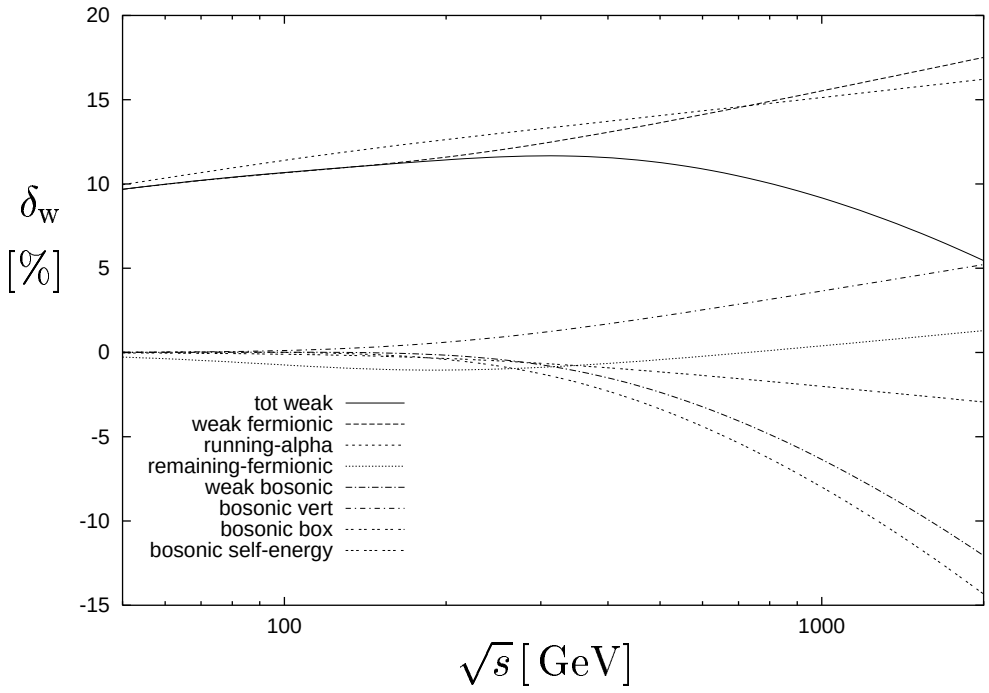

Fig. 2. Individual contributions to the relative weak corrections to the unpolarized differential cross section for $\vartheta = 90^\circ$

in Fig. 2 for a scattering angle of 90° and CM energies between 50 GeV and 2 TeV. The complete weak corrections are of the order 10% and vary slowly with energy (in the range between +5.4% and +11.7%). For energies below the Z-boson mass they are dominated by the fermionic contributions, which grow logarithmically from 9.7% at 50 GeV to 17.5% at 2 TeV. The bulk of the fermionic corrections is due to the running of α (ranging between 10.0% and 16.2%), and the remaining fermionic corrections are less than 1.3% in the considered energy range. While the bosonic corrections are less than 1% below 300 GeV, they reduce the weak corrections considerably at higher energies, e.g. by 12% at 2 TeV. This reduction originates predominantly from the box corrections, more precisely from the boxes involving W-boson exchange. The weak vertex corrections yield a positive contribution (5.2% at 2 TeV) which is again dominated by the diagrams involving W bosons. Finally, the bosonic self-energy corrections contribute −2.9% at 2 TeV.

In order to allow for a detailed check of our calculations we present in Table 1 the differential and integrated lowest-order cross sections together with the relative electromagnetic and weak corrections split into fermionic and bosonic parts. The fermionic corrections are further divided into those originating from the running of α and the rest.

We recall that the electromagnetic corrections are evaluated in the soft-photon approximation and hence depend strongly on the soft-photon-energy cut-off which was set to $\Delta E = 0.05\sqrt{s}$. They are strongly reduced once hard bremsstrahlung is included.

In Figs. 3 and 4 we show the lowest-order cross sections and the corresponding relative weak corrections for various polarizations of the incoming electrons at the scattering angle $\vartheta = 90^\circ$ as a function of the CM energy. For $\sqrt{s} \gg M_{\rm Z}$, the lowest-order cross sections drop as $1/s$, and the ratios between different polarized cross sections are energy-independent [cf. (2.9)]. The relative corrections are about 10% for small energies and vary between -5% and 18% at 2 TeV depending on the polarization. Besides the complete weak corrections we show in Fig. 4 also the weak corrections that remain after the subtraction of the effects of the running α [see (5.4)]. These remaining weak corrections are small at low energies for all polarizations and for purely right-handed electrons at all energies. The large negative corrections for the other polarizations at high energies are due to vertex and box diagrams involving W-boson exchange, which contribute only for at least one or two left-handed incoming electrons, respectively. The small differences in the corrections for different polarizations at low energies are due to the γ–Z mixing-energy and to differences in the interference structures in (2.8).

Figures 5 and 6 illustrate the angular dependence of the polarized lowest-order cross sections and the corresponding corrections, respectively. Owing to Fermi symmetry the cross sections are forward–backward symmetric, and it is sufficient to consider the forward direction. In the very forward direction the lowest-order cross section turns into the Rutherford cross section that diverges for $\theta \to 0$ like $1/t^2$ and is independent of the polarization of the incoming electrons. As can be seen from (2.9), for high energies and not too small scattering angles ($|t| \gg M_{\rm Z}^2$), the ratio between the different polarized lowest-order cross sections takes a particularly simply form. Thus, the ratio of LL to RR is constant and roughly equal to one, and the ratio of LR to RR decreases from 1 at $\vartheta = 0^\circ$ to 1/32

Table 1. Lowest-order cross sections and relative corrections for unpolarized particles

$\sqrt{s}$ [GeV]	ϑ	$\left(\frac{\mathrm{d}\sigma}{\mathrm{d}\Omega}\right)_{\mathrm{Born}}$ [pb]	δ_{em} [%]	δ_{w} [%]	$\delta_{\mathrm{w,bos}}$ [%]	$\delta_{\mathrm{w,fer}}$ [%]	$\delta_{\mathrm{w,run}}$ [%]	$\delta_{\mathrm{w,fer,rem}}$ [%]
	10°	36001	−26.95	6.98	−0.00	6.98	6.99	−0.01
	30°	476.75	−30.22	9.25	−0.01	9.25	9.36	−0.11
100	90°	23.024	−32.82	10.68	0.02	10.66	11.40	−0.74
	$10^\circ < \vartheta < 90^\circ$	3461.1	−28.42	7.98	−0.00	7.99	8.05	−0.06
	$30^\circ < \vartheta < 90^\circ$	402.08	−31.39	9.96	−0.00	9.96	10.27	−0.32
	10°	1452.9	−31.59	10.03	−0.19	10.22	10.36	−0.14
	30°	21.326	−34.85	10.89	−1.16	12.05	12.67	−0.62
500	90°	1.2366	−37.31	11.27	−2.36	13.63	14.06	−0.43
	$10^\circ < \vartheta < 90^\circ$	145.61	−33.13	10.53	−0.60	11.13	11.45	−0.33
	$30^\circ < \vartheta < 90^\circ$	19.533	−36.02	11.00	−1.76	12.77	13.37	−0.60
	10°	98.713	−35.58	8.27	−4.29	12.56	13.15	−0.59
	30°	1.4375	−38.78	5.11	−10.04	15.16	15.11	0.05
2000	90°	0.07957	−41.07	5.46	−12.05	17.51	16.21	1.30
	$10^\circ < \vartheta < 90^\circ$	9.9259	−37.08	6.80	−6.95	13.74	14.07	−0.33
	$30^\circ < \vartheta < 90^\circ$	1.2867	−39.88	5.02	−11.23	16.25	15.68	0.57

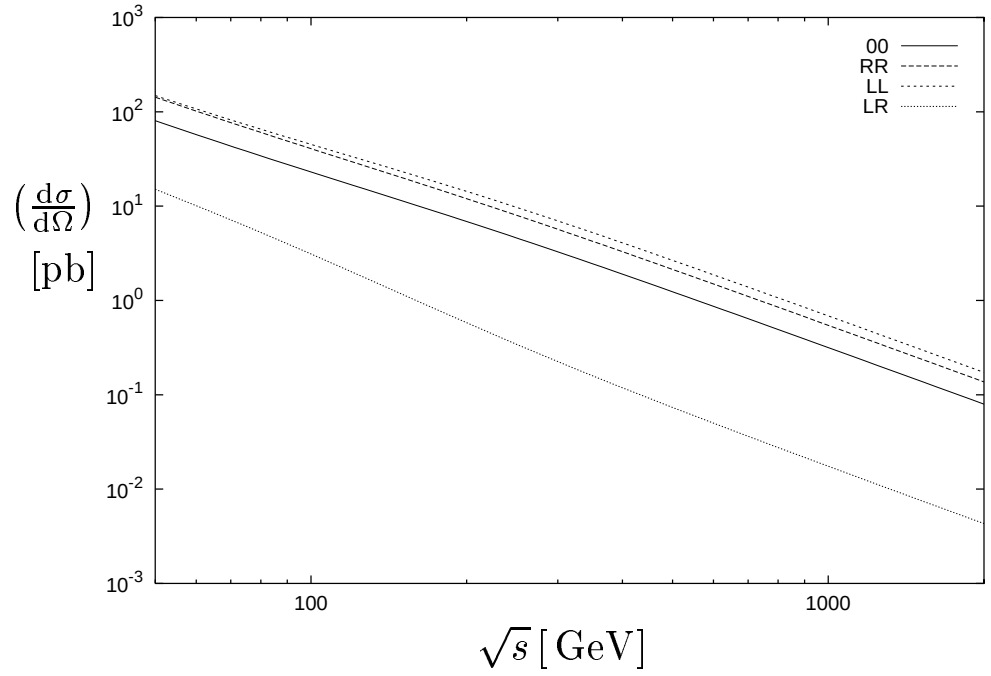

Fig. 3. Unpolarized (00) and polarized (RR,LL,LR) differential cross sections in Born approximation ($\vartheta = 90^\circ$)

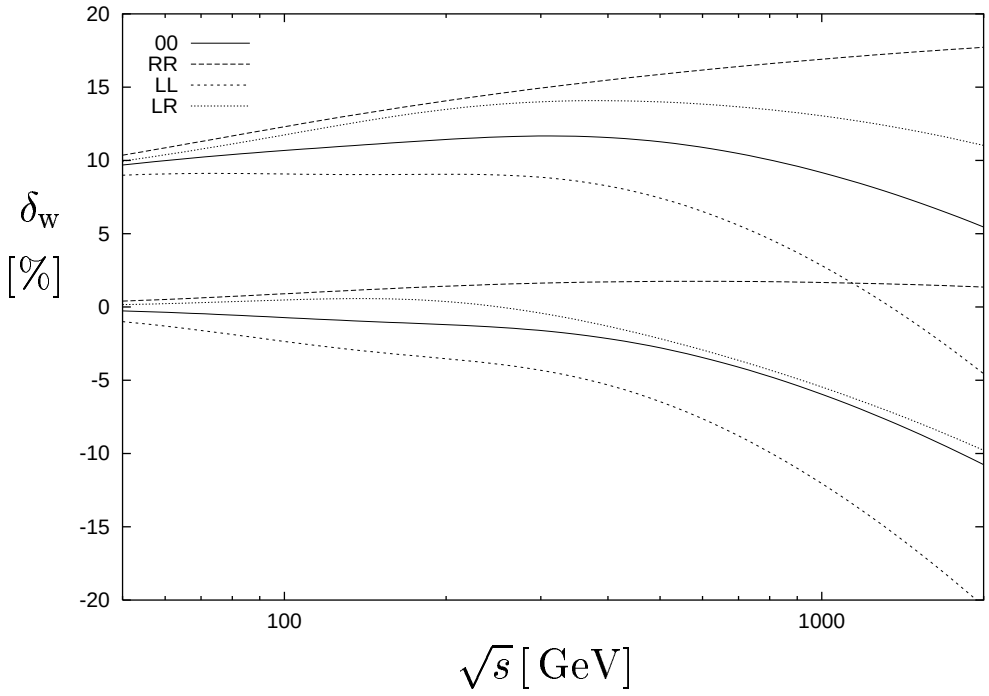

Fig. 4. Relative weak corrections to the unpolarized (00) and polarized (RR, LL, LR) differential cross sections including (*upper curves*) and excluding (*lower curves*) the effect of the running α ($\vartheta = 90^\circ$)

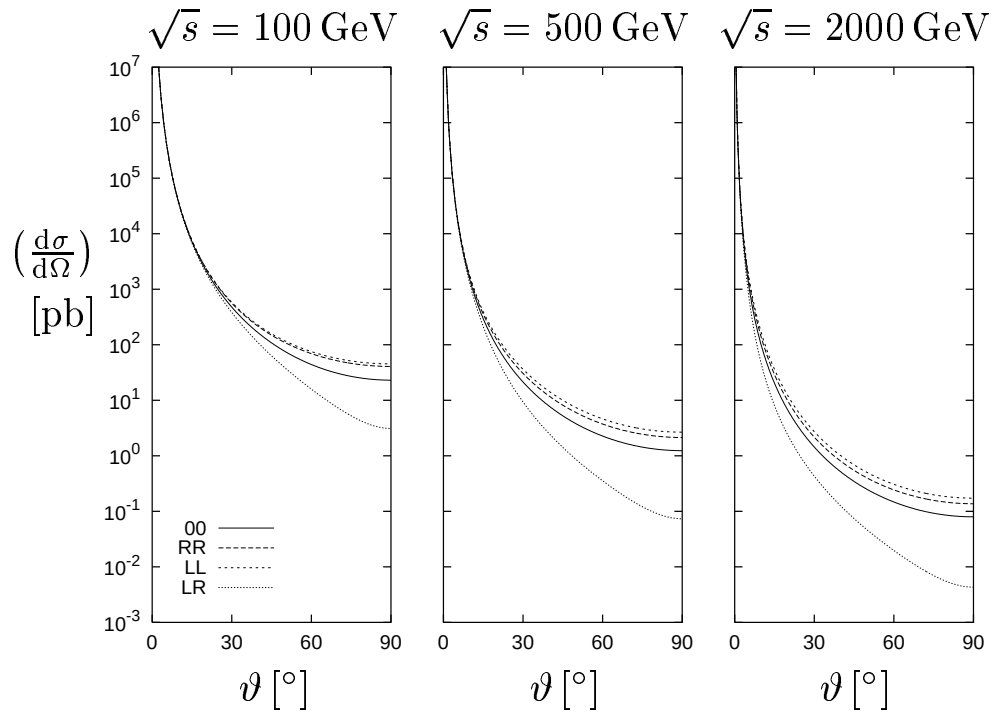

Fig. 5. Unpolarized (00) and polarized (RR,LL,LR) differential Born cross section as a function of the scattering angle ϑ for different CM energies

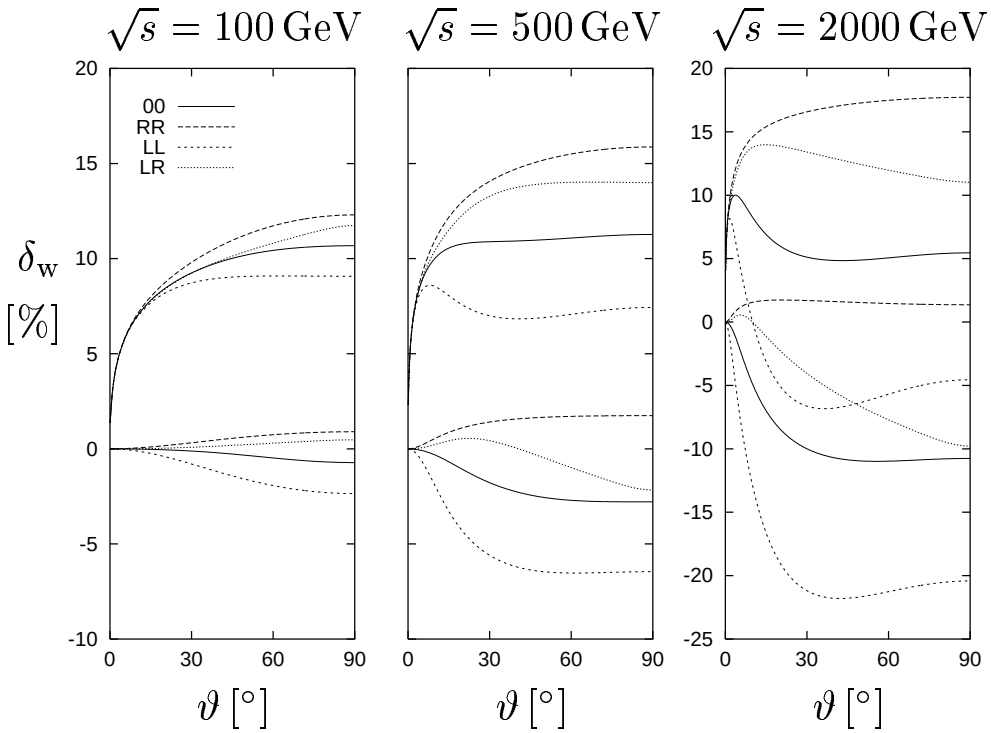

Fig. 6. Relative weak corrections to the unpolarized (00) and polarized (RR,LL,LR) differential cross sections as a function of the scattering angle ϑ for different CM energies including (*upper curves*) and excluding (*lower curves*) the effects of the running α

at $\vartheta = 90°$. The relative weak corrections vanish exactly in the forward direction. This can be explained as follows: In the forward direction, the lowest-order cross section is determined solely by the t-channel photon-exchange diagram which involves the $1/t$ pole. Similarly, only corrections that involve this pole are relevant, i.e. the self-energy and vertex corrections to the dominating lowest-order diagram. However, at the pole the virtual photon in these diagrams becomes real and these corrections vanish owing to the on-shell renormalization condition for the electric charge. For finite scattering angles, the weak corrections and their composition behave roughly as for the case of 90° scattering discussed above.

In Figs. 7 and 8 we show the differential polarization asymmetries $A_\mathrm{LR}^{(k)}$, $k = 1, 2, 3$, in Born approximation and including weak one-loop corrections. The lowest-order asymmetries are very small for low energies, grow in the energy range where $|t| \sim M_\mathrm{Z}$ and approach constant values for $|t| \gg M_\mathrm{Z}$. For $A_\mathrm{LR}^{(3)}$ the asymptotic value is independently of the scattering angle given by $(1-16s_\mathrm{w}^4)/(1+16s_\mathrm{w}^4) \approx 0.1156$. The three asymmetries have similar energy dependence, and $A_\mathrm{LR}^{(2)}$ is close to $A_\mathrm{LR}^{(3)}$ in particular for $\vartheta = 90°$. The relative complete weak corrections, shown in Fig. 8, are practically equal for all three asymmetries (the three curves in Fig. 8 can hardly be distinguished) and are about -40% for energies up to a few hundred GeV. In this regime the asymmetry is mainly due to the γ–Z mixing energy, while the effect of the running α (which is included in Fig. 8) cancels to a large extent. Owing to the strong parity-violating effects of the weak bosonic corrections the asymmetries are even further reduced at higher energies and reverse sign above about 2 TeV. The large corrections to the asymmetries arise from the fact, that many of the weak corrections like the γ–Z mixing energy or the contributions involving virtual W bosons are not suppressed by $1 - 4s_\mathrm{w}^2$ as the lowest-order asymmetries [8]. As a consequence these corrections are enhanced by a factor of about 10 in the asymmetries. Some numerical results for the asymmetries $A_\mathrm{LR}^{(k)}$ in lowest-order approximation and including the weak corrections are listed in Table 2. As illustrated in Fig. 8, the purely electromagnetic corrections affect the asymmetries only weakly.

For $s = 0.05\,\mathrm{GeV}^2$ and $\vartheta = 90°$ Czarnecki and Marciano have found corrections to the asymmetry $A_\mathrm{LR}^{(3)}$ of $-40 \pm 3\%$ using the $\overline{\mathrm{MS}}$ scheme, taking the Fermi constant G_μ as input, and including electromagnetic corrections. Translating this result to the on-shell scheme with M_W as input by using the relations given in [15] and subtracting the electromagnetic corrections yields -49% whereas we find -48% in good agreement.

6 Summary

We have calculated the $O(\alpha)$ radiative corrections to the process $\mathrm{e^-e^-} \to \mathrm{e^-e^-}$ within the Electroweak Standard Model using the soft-photon approximation for real photon emission. All relevant analytical results for the corrections to the polarized cross section have been given. The corrections have been split in a gauge-invariant way into electromagnetic and weak ones, and we have focused on the weak corrections.

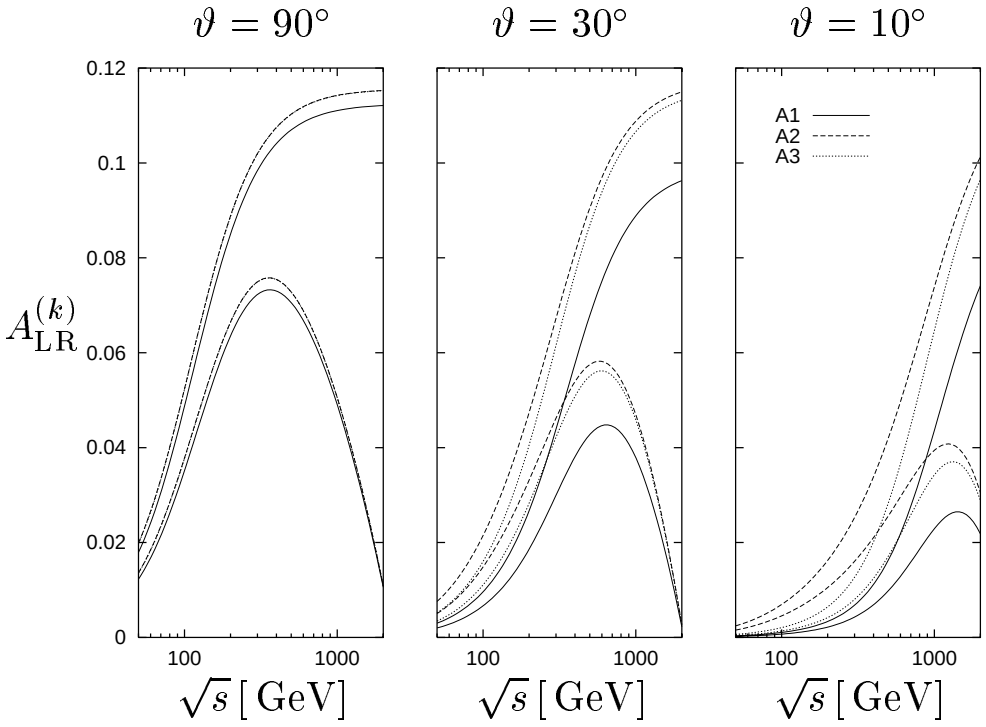

Fig. 7. Differential polarization asymmetries $A_{\mathrm{LR}}^{(k)}$ in Born approximation (*upper curves*) and including the complete weak one-loop corrections (*lower curves*) for different scattering angles

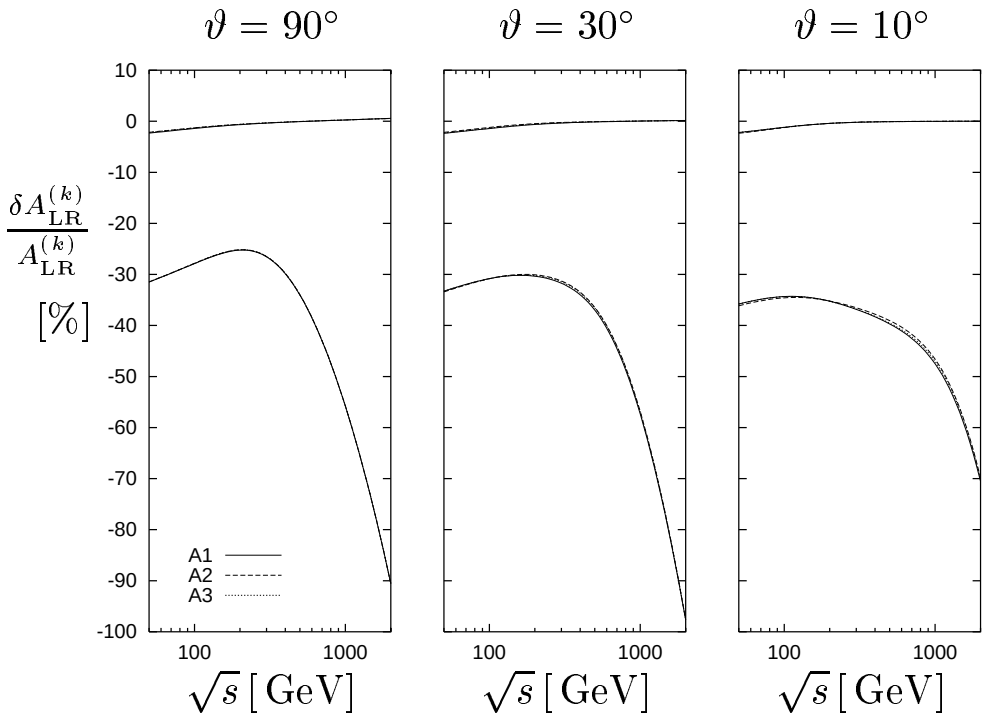

Fig. 8. Relative complete weak (*lower curves*) and electromagnetic (*upper curves*) one-loop corrections to the differential polarization asymmetries $A_{\mathrm{LR}}^{(k)}$ for different scattering angles

Table 2. Left-right asymmetries in Born approximation $A_{\mathrm{LR,Born}}$ and including weak one-loop corrections $A_{\mathrm{LR,w}}$ in units of 10^{-3}

$\sqrt{s}$ [GeV]	ϑ	$A^{(1)}_{\mathrm{LR,Born}}$	$A^{(1)}_{\mathrm{LR,w}}$	$A^{(2)}_{\mathrm{LR,Born}}$	$A^{(2)}_{\mathrm{LR,w}}$	$A^{(3)}_{\mathrm{LR,Born}}$	$A^{(3)}_{\mathrm{LR,w}}$
	10°	1.058	0.695	6.934	4.536	2.067	1.357
	30°	9.610	6.648	21.46	14.84	16.01	11.07
100	90°	48.72	35.14	52.39	37.81	52.25	37.71
	$10^\circ < \vartheta < 90^\circ$	5.042	3.536	15.77	11.00	9.149	6.410
	$30^\circ < \vartheta < 90^\circ$	23.33	16.60	34.94	24.84	32.27	22.95
	10°	16.33	9.848	42.08	25.65	28.39	17.16
	30°	67.89	42.77	90.53	57.52	86.91	55.08
500	90°	107.0	70.55	110.3	72.80	110.2	72.77
	$10^\circ < \vartheta < 90^\circ$	38.66	24.19	66.82	42.15	57.93	36.39
	$30^\circ < \vartheta < 90^\circ$	87.16	55.93	101.6	65.49	100.4	64.68
	10°	74.12	21.84	101.3	30.53	96.54	28.89
	30°	96.26	2.246	115.0	2.730	113.2	2.679
2000	90°	112.1	10.58	115.3	10.89	115.2	10.89
	$10^\circ < \vartheta < 90^\circ$	86.06	14.04	109.1	18.16	106.1	17.57
	$30^\circ < \vartheta < 90^\circ$	102.9	3.421	115.1	3.866	114.4	3.837

The weak corrections to the unpolarized cross section are typically of the order 10%. After subtracting the effect of the running of the electromagnetic coupling constant, the remaining corrections are small at low energies. The corrections to the cross section for purely right-handed electrons are dominated by the fermion-loop contribution to the gauge-boson self-energies, in particular by the contributions associated with the running electromagnetic coupling, and grow logarithmically with the centre-of-mass energy. For left-handed electrons the corrections involve in addition vertex and box diagrams with virtual W bosons, which yield sizeable negative corrections at energies higher than the Z-boson mass.

The polarization asymmetry, which ranges between 0 and 0.12 in lowest order, gets relative corrections of the order -40% for CM energies up to 500 GeV. For higher energies the parity-violating corrections increase fast and change the sign of the asymmetry above 2 TeV.

References

1. C. Møller, Annalen der Physik **14**, 531 (1932)
2. F. Cuypers, P. Gambino, Phys. Lett. **B388**, 211 (1996)
3. A. Czarnecki, W.J. Marciano, BNL-HET-98/4, hep-ph/9801394
4. M.L.G. Redhead, Proc. Roy. Soc. **A220**, 219 (1953); R.V. Polovin, J. Exptl. Theoret. Phys. **31**, 449 (1956) Soviet Phys. JETP **4**, 385 (1957); Y.S. Tsai, Phys. Rev. **120**, 269 (1960)
5. R. Gastmans, Y. Van Ham, Phys. Rev. **D10**, 3629 (1974); L.L. DeRaad, Jr., Phys. Rev. **D11**, 3328 (1975); L.L. DeRaad, Jr., Y.J. Ng, ibid. **D11**, 1586 (1975)
6. S. Jadach, B.F.L. Ward, Phys. Rev. **D54**, 743 (1996)
7. N.M. Shumeiko, J.G. Suarez, hep-ph/9712407
8. A. Czarnecki, W.J. Marciano, Phys. Rev. **D53**, 1066 (1996)
9. M. Böhm, A. Denner, W. Hollik, Nucl. Phys. **B304**, 687 (1988)
10. S. Weinberg, Phys. Rev. Lett. **19**, 1264 (1967); A. Salam, in *Elementary Particle Theory*, ed. N. Svartholm (Stockholm, 1968) p. 367; S.L. Glashow, J. Iliopoulos, L. Maiani, Phys. Rev. **D2**, 1285 (1970)
11. M. Böhm, W. Hollik, H. Spiesberger, Fortschr. Phys. **34**, 687 (1986)
12. A. Denner, Fortschr. Phys. **41**, 307 (1993)
13. S. Eidelman, F. Jegerlehner, Z. Phys. **C67**, 585 (1995)
14. H. Burkhardt, B. Pietrzyk, Phys. Lett. **B356**, 398 (1995)
15. Particle Data Group (R.M. Barnett et al.), Phys. Rev. **D54**, 1 (1996)